Aquatic Insect Populations' Responses to Time-Varying Reproductive Rates

Sarah Hinton, Ethan Levien, Zach Siegel
EISI - Oregon State University

August 22, 2012

1 Introduction

1.1 Objective and Motivation

'Drift', or dispersal, in the context of aquatic entomology, is the process of an individual detaching from the benthos to enter the water column and relocate within a river stretch. Populations face the 'drift paradox', which is the question of how upstream populations are able to persist when they are being drifted downstream. The treatment of this paradox is a defining feature of models of populations on a river stretch (Lutscher 2005). The potential of these models to forecast population stability is desirable because aquatic insect populations are indicators for the health of stream ecosystems. Identified causes of insect drift are described in papers (Huryn, 2000; Allan, 1989; Gibbons, 2010; Breitenmoser-Wursten, 1994), though little is known regarding how long and how far insects drift. Progress has been made into the effects of dispersal on the persistence of populations within mechanistically-derived models that have assumed drift to be an 'advection-diffusion' process, which is equivalent to diffusion by Brownian-motion of chemicals within a unidirectional flow (Lutscher 2005, Ramirez 2011). Necessary conditions for population persistence have been determined under these assumptions; however, the gap between biological data and mathematical models has limited their predictive ability.

A main focus of this paper is the use of quantitative and qualitative data, both accepted in published literature and collected experimentally, to parameterize numerical simulations of existing models. The findings of this paper consist of reconciliations of the outputs of mathematical models with an understanding of the physical and biological behavior of aquatic organisms in a river stretch.

Data was collected from field experimentation to determine the dispersion kernel for aquatic insects. Aspects of the model were computationally parameterized for a 'best-fit' with the goal of comparing the fit to the collected data (under the assumption of the 'advection-diffusion' model). In turn, the accuracy

of the optimal parameterization could be examined by comparison to measurable quantities, such as average stream velocity. In these ways, the correlation between relatively mature models and complex biological systems can be better understood.

1.2   Prior Research

Though aquatic insect dispersal has been studied since the early 20th century, little is known about the mechanisms involved in dispersal. In 1972, Thomas Waters wrote a literature review summarizing the main research that had been conducted to that point. One point that is most agreed on is the diel periodicity of aquatic insect drift. The cause of this periodicity is unknown, although some research speculates it is related to predation. Research has shown that the presence of a predator may lead to reduced mobile activity, increased sheltering behavior, and greater nocturnal activity (Huryn 2000). Other research has been conducted to determine how factors such as body size, hunger (Allan 1989), gravel size (Gibbons 2010), and insect life cycle (Breitenmoser-Wursten 1994) relate to aquatic insect dispersal. In general, it is known that a starved animal will disperse more frequently than one that is not (Allan 1989). In the same research, it was also shown that a larger (more mature) insect will drift farther. This is correlated to the insect life cycle and also gravel size. The younger the insect, the greater its ability to attach to various sizes of sediment (Gibbons 2010). Insect life cycle is one of the largest contributing factors to drift because an insect will drift only during the nymph phase of its life cycle. It is shown that a nymph will drift due to the fact that it is looking for a place to emerge as an adult (Waters 1972). All of these factors are important considerations to develop an appropriate mathematical model, but not every factor can be included for the sake of simplicity. This lack of accuracy is shown in the mathematical models have been attempted to date. These models attempt to show dispersion through partial integro-differential equations of advection-diffusion processes (Lutscher 2005, Ramirez 2011), but little has been done to test the parameterization of these models in a true biological setting.

1.2.1   Defining Parameters from Prior Research

There are constants included in the mathematical model are extremely difficult to calculate in the field. Thus, literature values were identified for the following environmental parameters: reproductive growth rate (the variable r), aquatic insect life cycles, and time of day. The insects chosen for all numerical values derived from the literary research are of the genus Baetis. To find r, the raw number of eggs deposited per female was used. This number was approximately 200-3000 eggs/female (Encalada 2005). Because the number of new adult insects per year per original insect was needed, the mortality at each life stage was found. These numbers were approximately 10-20% mortality for eggs, and 95% mortality for all other insects that do not reach the reproduction age (Huryn 2000). Insect drift is minimally affected by time of day, such

as by diel periodicity, predation, hunger (Waters 1972), and stage in life cycle (Breitenmoser-Wursten 1994).

1.3 Mathematical Model

The model used throughout this research is adopted from the model described in Ramirez (2011). It considers a species in a one dimensional stream where an individual may be in one of two states at any given time: drifting in the water, or attached to the bottom. During periods of drift it is assumed that individuals are transported by means of an advection diffusion process. This assumption is consistent with previous experimental and analytical research (Fischer, 1973; Lutscher, 2005; Ramirez, 2011). During periods when an individual is attached to the bottom they remain stationary. Individuals grow per capita at a time dependent rate which may be negative or positive. Transport by drift, and death through a negative growth per capita are the only mechanisms able to remove individuals from the system.

1.4 Study Site

Research was conducted July 18-19, 2012 at Watershed 3 (WS3) at H.J. Andrews Experimental Forest (HJA), located in the Willamette National Forest (Oregon Cascades). HJA is a Long-Term Ecological Research (LTER) site funded by the National Science Foundation. It has been used for many types of ecological research and experiments. HJA has a complex network of rivers and streams contained within watersheds. The study site for our experiment was a second order stream in Watershed 3 (WS03) that empties into Lower Lookout Creek (Andrews Website). We selected a reach within WS3 that had relatively constant vegetative cover, soil composition, bedrock, gradient, channel cross-sectional area, turbidity, and velocity. An 18-meter reach that was bedrock dominated with a width of approximately 1.7 meters, a depth of .5 meters and a velocity measured in the main channel of flow of .35 m/s was chosen for field measurements. This reach was also chosen because the consistent features are easy to model and due to the complexities of creating a flume capable of replicating the nuances of a natural system. In addition, the consistent features can be generalized as constants within the mathematical model. Another important aspect of this stream was the narrow channel width, which enabled the drift net to capture the majority of tracers without the addition of a more complex catching system.

2 Methods

2.1 Analytical Model

A population $u(x, t)$ on a stretch of river Γ with length l, growth per capita $r > 0$ per unit time and rate of mobility $\mu > 0$ at time $t > 0$ and upstream distance $x >$

3

0 can be modeled using the the following integro-differential equation described by Lutscher et al.(2005) and Ramirez (2011) :

$$\frac{\partial u}{\partial t}(x,t) = \left(\frac{r}{\mu} - 1\right) u(x,t) + \int_{y \in \Gamma} \mathcal{K}(y,x) u(x,t) dy. \tag{1}$$

The dispersion kernel $\mathcal{K}(y,x)$ describes the probability that a drifting individual disperses from y to x. Under the hypotheses considered by Ramirez (2011), the movement of individuals in the drift is modeled by an advection diffusion process, and an expression for $\mathcal{K}(y,x)$ under this assumption can be found using the method described in Appendix (6). Fig (1) plots changes in $\mathcal{K}(y,x)$ with respect to parameters of diffusion and velocity.

In Ramirez (2011) and Lutscher et al. (2005), the critical growth rate r_{crit} is defined to be the minimum reproduction per individual per unit time at which the zero-solution is unstable; with reproduction greater than r_{crit}, a nonzero population will not reduce to zero. The critical rate r_{crit} can be derived analytically in terms of the rate of mobility μ and properties of the dispersion kernel $\mathcal{K}$, specifically as stated in Appendix (5.3).

The existing model is generalized to accommodate time dependent reproductive rates; in this case (1) becomes

$$\frac{\partial u}{\partial t}(x,t) = \left(\frac{r(t)}{\mu} - 1\right) u(x,t) + \int_{y \in \Gamma} \mathcal{K}(y,x) u(x,t) dy. \tag{2}$$

Additionally, periods of population death are considered, meaning for some t, $r(t) < 0$.

The concept of a critical growth rate r_{crit}, while less precisely determined, is generalized to properties of time-dependent functions of growth and death, $r(t)$, for which a population will persist, one of which properties is R:

$$R(T) = \int_0^T r(t) dt. \tag{3}$$

2.2 Numerical Methods

In order to assess the sensitivity of a population to time varying reproductive rates, (2) was solved numerically. For all experiments , a population was simulated on a river stretch of length $l = 10$ meters with parameter values $D = 5.6$, $v = 0.21$, $\sigma = 100$, and $\mu = 1$. For these parameters the constant $r_{crit} = 0.97$ was computed using (15) . The following numerical experiments were run:

  i The analytical reproductive rate and the numerical model were reconciled by running simulations with constant reproductive rates varying between $r_{crit} - 0.4$, and $r_{crit} + 0.4$.

 ii The population's growth and decay over time, as well as its overall persistence, were observed under the following reproductive-rate functions $r(t)$:

4
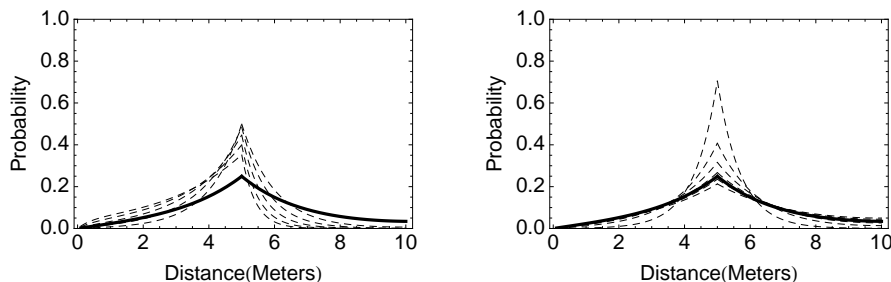
Figure 1: Probabilities of transition from y to a given x, $\mathcal{K}(y,x)$, plotted over a river stretch for varying values of v (left) and D (right)

- Spike in reproduction at one point in time, with zero reproduction otherwise (to simulate a breeding period in a year).
- Periodic impulses of reproduction with and without periods of death (in the form of a negative reproductive rate).
- Various rearrangements of a normal distribution of reproductive rates with a specified mean and standard deviation, with and without periods of death.

The model equation (1) for population along a river stretch scales arbitrarily, meaning that it can be used to indicate percentage of initial population at points along its domain. Thusly lacking discretization, it will not directly indicate a population's extinction or persistence, though these qualities can be inferred numerically. In simulations, a population that is substantially below its initial condition and is decreasing further will be considered extinct. In some cases it is appropriate to consider a cutoff for extinction and in other cases it is not. In addressing the time elapsed until extinction, the specific definition of extinction will be indicated.

All simulations were conducted using an implicit first-order solver. Time steps were rescaled such that for each time-step Δt_i at which $r(t_i) \geq 0.1$, the condition $r\Delta t_i = c$ was ensured for some constant c. When $r(t_i) < 0.1$, the condition became $\Delta t_i = c$. The Mathematica code used to run these simulations is available upon request from the authors.

All simulations were done using experimentally determined values for D, v and l. Other parameters used were σ and μ; under the assumption that an organism spends the majority of its life cycle stationary, out of the drift, values of σ were used that were around two orders of magnitude greater than those of μ. For simplicity, and without biological consideration, the values $\mu = 1$, $\sigma = 100$ were used in all experiments.

5

2.3 Parameter Determination

Field research was conducted to experimentally determine the dispersion kernel. The experiment was conducted with tracers made from flat toothpicks divided into quarters. Flat toothpicks were chosen because of their similarities to insects. The toothpicks were approximately insect shaped and had a near neutral buoyancy. Neutral buoyancy enabled the tracer to stay within the water column like an insect, without any effects of floating or sinking. Another important factor of using toothpicks is that they were easy to mark and recapture for identification later. Tracers were released from four different locations and four different times for a total of 16 data points. Each data point had a unique pattern marked onto the toothpick in order to count them after collection . A standard-sized drift net was placed near the end of the stream for the duration of the experiment. The drift net spanned 70% of the width of the channel and included the entire depth of the stream. Tracers that made it past the drift net, or that went around, were collected in a small net by hand and included in the tally of those collected by the drift net. For each release point and time, 80 tracers were used (20 toothpicks divided into quarters). The release points were defined as the distance from the drift net. The first release distance was at 10 meters, the next was at 12 meters, the third at 15 meters, and the farthest at 18 meters. At each release point, there was one person to release tracers in the stream in order to have an instantaneous process. The first tracers for each point were in the stream for a total of 960.0 seconds. The second group of tracers for each point were in the stream for 729.6 seconds. The third group of tracers were in the stream for 504.9 seconds, and the fourth group were in the stream for 189.6 seconds. After the last group had been in the water for the designated time, the drift net was pulled out of the water. Any tracers that had made it past the net were collected and included in the tally of those collected by the net. The tracers were taken out of the net, sorted, and hand counted. The results of the collection are summarized in Table (1).

The number of tracers collected from distance x after time t, $n_{x,t}$ out of the total number of tracers released from that distance for that amount of time, $N_{x,t}$, corresponds to

$$n_{x,t} = N_{x,t} \int_0^t \mathbb{P}(H_0^x \in dt(t))dt, \tag{4}$$

where H_0^x denotes the 'stopping time' for a tracer coming from distance x, which is the time it takes to be collected after traveling that distance. The specific expression for $\mathbb{P}(H_0^x \in dt(t))$ is derived in Appendix (7.1) in terms of D and v to be

$$\mathbb{P}(H_0^x \in dt(t)) = D\frac{\partial P}{\partial x}(y, 0, s) \tag{5}$$

under the assumption that the tracers involved are transported by means of an advection-diffusion process, where $P(y, x, t)$ denotes the probability of transitioning from location x to y at time t.
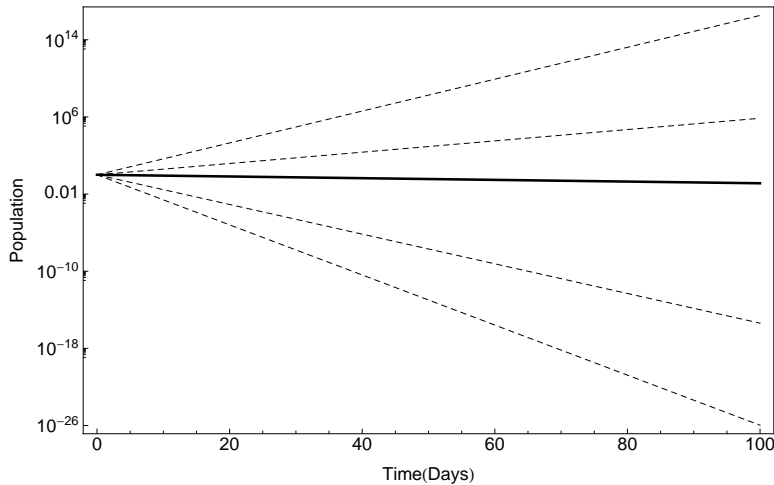
Figure 2: Results of experiment (i). The total percent of the initial population remaining on the river for populations with constant r values varying between $r_{crit} - 0.4$ and $r_{crit} + 0.4$.

The values of D and v were then determined using a least-squares fit.

The values obtained for D and v were then used in all subsequent experiments.

3 Results

3.1 Numerical Results

Numerical simulations produced the following results:

(i)

The numerical solver's correspondence with analytically-determined results was confirmed by observing that the analytically-determined r_{crit} was indeed the requirement for population-persistence under a constant reproductive function. This result is evident from Figure (2).

(ii)

It was found that a population with a non-increasing time-dependent reproductive function $r(t)$ is likely to have persisted until time T if

$$\int_0^T r(t)dt = R(T) \geq T \cdot r_{crit} \tag{6}$$

where R is explained in (3).
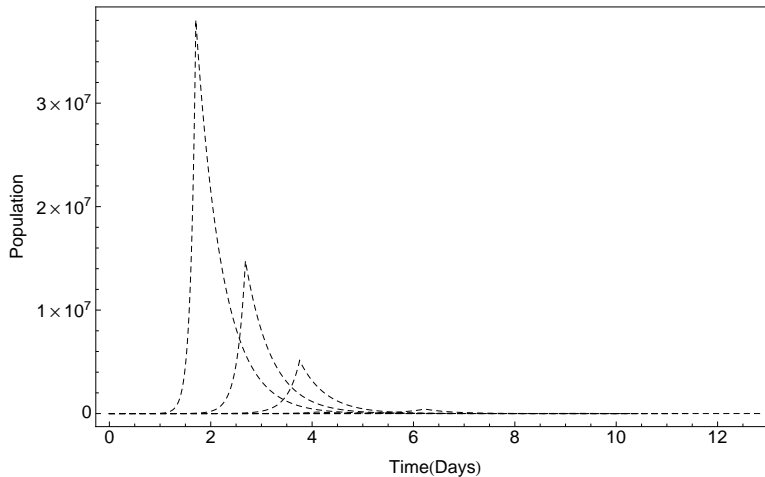
Figure 3: The total percent of the initial population remaining on the river for populations with reproductive impulses of durations varying between 1.6 and 3.2 days *at the beginning of the simulation*, and a death rate of 0.95 for the remainder of the simulation. In these simulations, (6) was maintained. This plot is for comparison to Figure (4).

Figure (3) displays the populations resulting from experiment (ii) in which reproductive rates with impulses of varying durations are compared to a constant reproductive rate of r_{crit}. It can be seen that all the populations converge to the same value at time T regardless of the initial reproductive impulse width provided (6) holds, implying that (6) is in fact a sufficient condition for persistence. These plots can be compared to those in Figure (4), in which an increase reproductive rate comes at the end of the simulation period. Together, these sets of plots explain the model's response to impulse-driven reproductive rates.

It was also found that a population with a time-dependent reproductive function $r(t)$ satisfying (6) will persist until time T if, for all intervals $[t_a, t_b] \in [0, T]$ such that $r(t) < r_{crit} \quad \forall t \in [t_a, t_b]$,

$$t_b - t_a < DT(min_{t \in (t_a, t_b)}[r(t)]). \tag{7}$$

$DT(c)$ approximately describes the time it takes for a given population with constant reproductive function $r(t) = c < r_{crit}$ to decrease below ten percent of its initial condition and can be approximated with a hyperbola as indicated in Figure (6).

The model's response to a normally-varying reproductive function with a specified mean and standard deviation was examined, and it was found that the deviations from the mean did not affect the persistence of the population; at a high resolution their effects on the population are evident, as can be seen in Figure (5)

Figure (6) displays numerical data used to determine the time-until-extinction
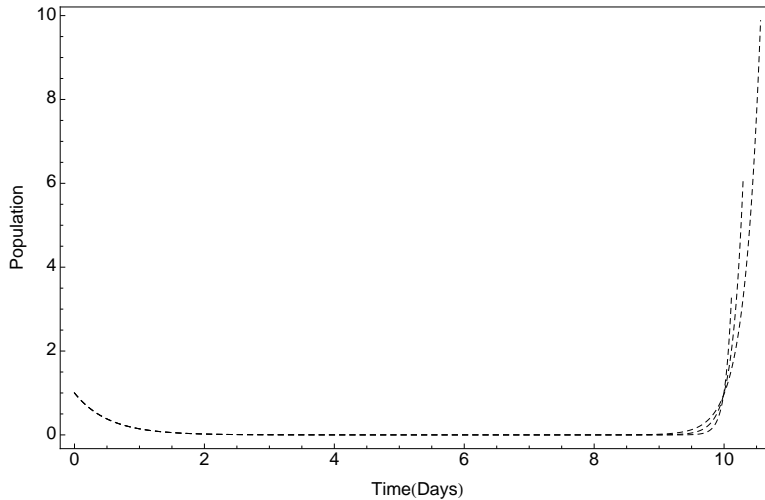
Figure 4: The total percent of the initial population remaining on the river for populations with reproductive impulses of durations varying between 1.6 and 3.2 days *at the end of the simulation*, and a death rate of 0.95 for the remainder of the simulation. In these simulations, (6) was maintained. This plot is for comparison to Figure (3).

$DT(r)$ for constant reproductive rates $r(t) = constant < r_{crit}$. Data points in (6) are fit to the curve $\frac{a}{b(r-c)}$ where $a = -1827.57$, $b = 769.15$ and $c = 1.00$. In a standard population-simulation utilizing the classical exponential-growth differential equation

$$rate\ of\ change\ in\ population \propto population,$$

time-until-extinction will fit a curve of this form. The close fit suggests that, in this respect, the effect of the advection-diffusion process is minimal.

3.2   Experimental Results

Through the tracer experiment outlined in section (2.3), values for advection velocity v and dispersion coefficient D were determined as those that most closely parameterized the model's correlation with observed data, as explained thoroughly in Appendix C (7).

The number of tracers collected, out of the total of 80 released from each spatio-temporal location, is given in Table (1).

The value of v determined by this process was $v = .21\frac{m}{s}$, whereas the measured value of the water velocity $0.35\frac{m}{s}$, as mentioned in the study's site-description (1.4). These numbers do not represent the same velocity, and should not be compared as such. The determined value of v is the mean velocity of a toothpick undergoing non-linear motion, and the measured velocity is the
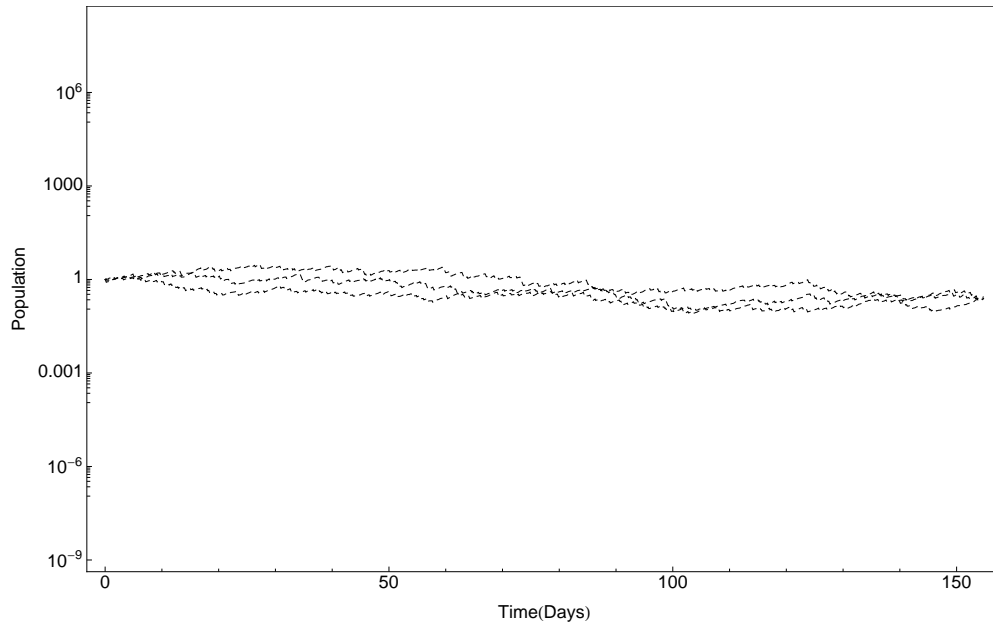
Figure 5: Numerical simulations with normally-distributed reproductive rates varying about a mean of the critical reproductive rate r_{crit}. The normal variation in reproductive function does not seem to effect the persistence of the population whatsoever.
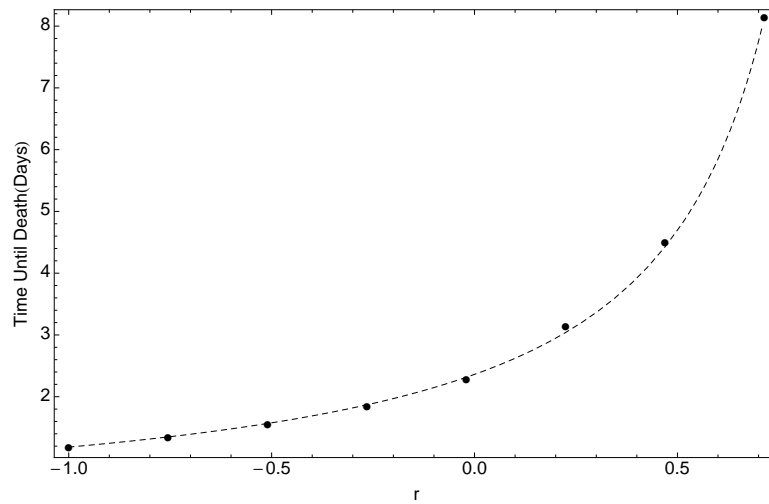
Figure 6: Numerically simulated time-until-extinction for constant reproductive rates varying between -1 and r_{crit}.

Time/Distance	10m	12m	15m	18m
190s	46	31	6	1
505 s	51	33	22	1
730s	68	30	13	1
960 s	52	28	22	1

Table 1: Number of tracers collected out of 80 released from various distances and timespans

velocity of an arbirarily chosen point within the stream. It is expected that the value of the determined velocity is less than the measured velocity due to measurements taken at a point of faster flow.

The value of the dispersion coefficient D obtained was $5.6\frac{m^2}{s}$; for reference, other tracer experiments in water have determined dispersion coefficients to be between 1 and $20\frac{m^2}{s}$ (Fischer, 1973).

4 Discussion

4.1 Biological Implications

The result of (i) demonstrates the accuracy of the numerical solution in that the analytically proven value of r_{crit} is indeed the critical constant reproductive rate for population persistence in the numerical simulations. Thus, the biological implications of the simulations are as relevant as any determined under the assumptions of the mathematical model governed by (1).

The results of (ii) quantify that a condition for persistence of a population with a general time-dependent reproductive rate is the total reproduction per individual per year. The implications of this are that populations of organisms reproducing throughout a given year and those reproducing all at one point in a given year are predicted by the model to have equal likelihoods of persistence; e.g. the number of eggs laid in a year is more important than the timing of the laying of the eggs. While the truth of such a conclusion within a biological system is questionable due to unexamined factors (such as an environment's limiting response to an abundance of individuals), it does point out that the effects of an advection-diffusion process alone cannot enforce a reproductive schedule necessary for the persistence of a population.

As noted in the methods, the model never indicates a population of zero, as it merely gives a percentage of the initial population remaining at a given time. Thus, to discuss the time elapsed until extinction, it must be noted that extinction is being defined as less than 10% of the initial population. Regardless of the assumptions employed, the value of $DT(r)$, the time it takes for a population to go extinct at a given reproductive rate $r < r_{crit}$, is relevant.

11
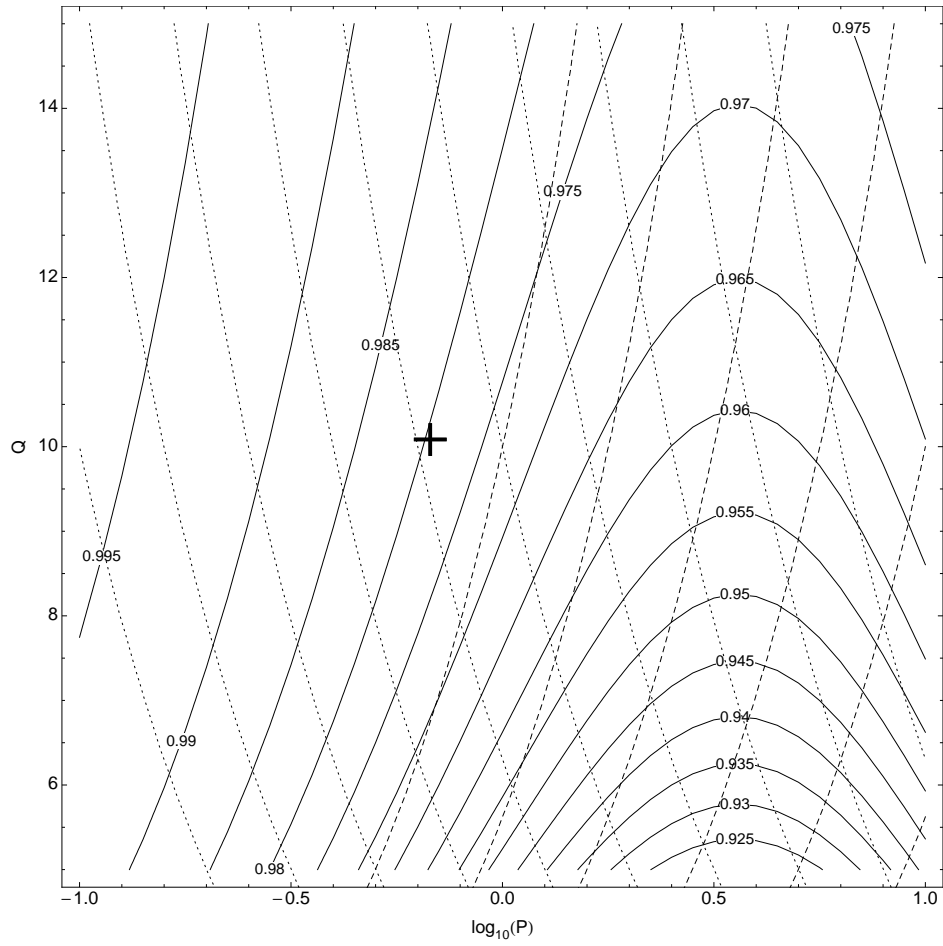
Figure 7: Contour plot for QP(dotted lines), Q/P(dashed lines) and $\frac{r_{crit}}{\mu}$(solid lines) with the experimentally determined values for Q and P plotted as a cross. The values used for σ and μ were 100 and 1, respectively.

4.2   A representative river stretch

Experimentally determined values of dimensionless quantities P and Q are explored through a contour plot in Figure (7). P and Q are defined as

$$P = \frac{vl}{D} \tag{8}$$

$$Q = \frac{v}{\sigma l} \tag{9}$$

where the Peclét Number P is seen in Appendix A (15), σ is the mean rate of exiting the advection and attaching to the benthos, D is the dispersion coefficient, v is the advection velocity, and l is the length of the river stretch. Observing that PQ results in the cancellation of the l term and $\frac{Q}{P}$ results in the cancellation of the v term allows us to examine the sensitivity of a given population's $\frac{r_{crit}}{\mu}$ value to changes in l or v. In the experimentally determined case the population will be less sensitive to increases in v which move the plotted point along the dashed lines producing little change in $\frac{r_{crit}}{\mu}$. Decreasing l, however, will move the point along the dotted lines increasing $\frac{r_{crit}}{\mu}$ at a steeper rate. Biologically, this means that streams similar to the one plotted will require similar lengths if they are to maintain an population, while their velocities may be more variable. The usefulness of this quantification is elaborated in Ramirez (2011).

4.3   Future Research

Future research may expand upon these results by considering the effects of time dependent reproductive rates on populations in dendritic networks. This paper, as well as previous analytical research on population dynamics in riverine settings hypothesizes that the transport of individuals in even such complex environments can be accurately modeled as an advection-diffusion process. Confirmation of this hypothesis would require a larger experimental data set as well as a deeper study of the dynamics governing organism drift.

Further exploration may also be made into a space-varying reproductive function $r(x,t)$. This might have a biological motivation if insects are found to lay their eggs preferentially in certain locations or generally upstream, a plausible notion.

Further analytical quantifications of time- and/or space-varying reproductive functions' 'critical quality' can be explored, as this paper has only tested a few such properties (e.g. R in (3)).

Another important area of consideration for future research is for the comparison of determined values of v with the mean velocity of the stream. In this research, we compared the best-fit velocity with the velocity measured at a single point in the part of the water column with highest flow, which is not comparable to the velocity of a toothpick undergoing advection motion. However, the motion of such a tracer might be comparable to the mean flow velocity over the cross-sectional area of the water column, which would be measured

by dividing discharge by the cross-sectional area of the stream. This would be easiest to perform on a stretch of stream with a discharge-gauging station.

5   Appendix A: Explanation of the Model

5.1   Model Explanation

The population's governing integro-differential equation (1) comes from the following equation

$$\frac{\partial u}{\partial t}(x,t) = ru - \mu u(x,t) + \mu \int_{\Gamma} \mathcal{K}(y,x)u(x,t)dy \tag{10}$$

with a change of variables to $t_{new} = \mu t_{old}$.

5.2   The Dispersion Kernel

COMBINE THIS WITH SECTION (6)

The dispersion kernel $\mathcal{K}(y,x)$ of equation (1), which describes the probability that a drifting individual will disperse from position y to x, is given by the expression

$$\mathcal{K}(y,x) = \int_0^{\infty} \sigma e^{-\sigma t} P(y,x,t)dt, \tag{11}$$

where σ is the probability of a mobile individual attaching to the bottom from the water column, and $P(y,x,t)$ is the probability that an individual will have transitioned from y to x in a time interval t and is the solution to the advection diffusion equation:

$$\frac{\partial P}{\partial t}(y,x,t) = D\frac{\partial^2 P}{\partial y^2}(y,x,t) - v\frac{\partial P}{\partial y}(y,x,t) \tag{12}$$

subject to boundary conditions $P(0,x,t) = \frac{\partial P}{\partial t}(l,x,t) = 0$.

5.3   Value of r_{crit}

As explained in Ramirez (2011) and Lutscher et al. (2005), the constant critical growth rate r_{crit} of a population can be derived in terms of the dispersion kernel $\mathcal{K}$ and the rate of mobility μ in equation (1)

$$\frac{\partial u}{\partial t}(x,t) = \left(\frac{r}{\mu} - 1\right)u(x,t) + \int_{y\in\Gamma} \mathcal{K}(y,x)u(x,t)dy. \tag{1}$$

Specifically,

$$r_{crit} = \mu(1 - \omega_{\mathbf{K}}), \tag{13}$$

where $\omega_{\mathbf{K}}$ is the largest eigenvalue of the operator

$$\mathbf{K}[f] = \int_{\Gamma} \mathcal{K}(y,x)f(y)dy. \tag{14}$$

14

Definition (13) can be understood intuitively by the fact that the critical growth rate represents the smallest growth rate at which the population can persist (read: can have non-negative derivative with respect to time) for some population distribution, however populous or scarce. Thus, when $r = r_{crit}$, by definition, we observe $\frac{\partial u}{\partial t} = 0$. We examine a non-zero population distribution $u(x,t)$ at equilibrium for which $\mathbf{K}[u] = \omega_{\mathbf{K}} \cdot u$, the most population-preserving distribution possible:

$$
\begin{aligned}
0 &= \frac{\partial u}{\partial t}(x,t) \\
&= \left(\frac{r}{\mu} - 1\right) u(x,t) + \int_{y \in \Gamma} \mathcal{K}(y,x) u(x,t) dy \\
&= \left(\frac{r}{\mu} - 1 + \omega_{\mathbf{K}}\right) u(x,t).
\end{aligned}
$$

Here, by definition, $r = r_{crit}$, the minimum possible value of r such that $\frac{\partial u}{\partial t} \geq 0$. Thus,

$$
\begin{aligned}
0 &= \left(\frac{r}{\mu} - 1 + \omega_{\mathbf{K}}\right) u(x,t) \\
\Rightarrow 0 &= \left(\frac{r}{\mu} - 1 + \omega_{\mathbf{K}}\right) \\
\Rightarrow r_{crit} &= r = \mu(1 - \omega_{\mathbf{K}}), .
\end{aligned}
\tag{13}
$$

It is shown in Ramirez (2011) that, for the specific dispersion kernel $\mathcal{K}$ resultant of the chosen boundary conditions of the model used in this paper, $\omega_{\mathbf{K}} = \frac{1}{\nu}$ where ν is the smallest solution solution to

$$
tan(l \cdot b(\nu)) + 2\frac{l \cdot b(\nu)}{P} = 0, \quad b(v) = \frac{1}{2D}\sqrt{v^2 - 4D\sigma(\nu - 1)}
\tag{15}
$$

such that $\nu \geq 1$, where P is defined as the Peclét number $P = \frac{v \cdot l}{D}$, a dimensionless quantity comparing the importance of advection to diffusion in dispersion (Ramirez, 2011).

Here, $\omega_{\mathbf{K}}$ is a function of the length of the river stretch l, velocity of advection v, and diffusion coefficient D. As discussed at length in Lutscher et al. (2005), this results in a 'critical domain size' and 'critical advection velocity,' which are computed. Implications regarding the value of r_{crit} due to various changes to the model's diffusion coefficient and boundary conditions are also discussed.

6 Appendix B: Finding the Dispersion Kernel $\mathcal{K}$

6.1 An identity derived from the Advection-Diffusion Equation Solution

We have seen SHOW IT IN SOME SECTION AND CITE IT HERE! that the solution to the advection diffusion equation

$$\frac{\partial p}{\partial t} = D\frac{\partial^2 p}{\partial x^2} - v\frac{\partial p}{\partial x},$$

which we denote $p(x, y, t)$, is the probability density function representing probabilities of traveling through a linear flow from point x to point y after time t.

The probability density function for a mobile individual to move from x to y over *all* t, taking into consideration the fact that the individual will exit the channel (attach, in the case of insects) at rate σ, is then given by

$$\mathcal{K}(x, y) = \int_0^\infty \sigma e^{-\sigma t} p(x, y, t) dt. \tag{16}$$

We leave behind our analytic solution for p and aim to derive $\mathcal{K}$ in a different way.

First, define the operator

$$\mathcal{A}[g](x) = Dg''(x) - vg'(x), \tag{17}$$

so that the advection-diffusion equation now states

$$\frac{\partial p}{\partial t} = \mathcal{A}[p] \tag{18}$$

Now, assuming $\mathcal{K}$ is integrable, we take $\mathcal{A}[\mathcal{K}]$

$$
\begin{aligned}
\mathcal{A}[\mathcal{K}(x, y)] =& \mathcal{A}[\int_0^\infty \sigma e^{-\sigma t} p(x, y, t) dt] \\
=& \int_0^\infty \sigma e^{-\sigma t} \mathcal{A}[p(x, y, t)] dt \text{ because integration w/r/t } t \text{ and differentiating w/r/t } x \text{ are linear} \\
=& \int_0^\infty \sigma e^{-\sigma t} \frac{\partial p}{\partial t} dt \text{ by (18)} \\
=& \sigma e^{-\sigma t} p(x, y, t)\big|_0^\infty - \int_0^\infty \sigma(-\sigma e^{-\sigma t}) p(x, y, t) dt \text{ by integrating-by-parts} \\
=& \sigma \delta_x(y) + \sigma \mathcal{K}(x, y) \tag{19}
\end{aligned}
$$

where $\delta_x(y)$ is the Dirac delta function[1].

Now, we move terms and define a new operator based on $\mathcal{A}$

$$(\sigma - \mathcal{A})[f] = \sigma f - \mathcal{A}[f]. \tag{20}$$

Now, (19) states that

$$(\sigma - \mathcal{A})[\mathcal{K}(x, y)] = \sigma \mathcal{K}(x, y) - \mathcal{A}[\mathcal{K}(x, y)] = \sigma \delta_x(y).$$

---

[1] $\sigma e^{-\sigma t} p(x, y, t)\big|_0^\infty = \sigma \delta_x(y)$ because $\lim_{t \to \infty} e^{-\sigma t} p(x, y, t) = 0$ and $\lim_{t \to 0} e^{-\sigma t} p(x, y, t) = \sigma \delta_x(y)$, which just means that at time $t = 0$, there is zero probability that any mobile individual moves from any point x to any point y unless $x = y$, and so we have a spike of probability mass (Delta function) along $x = y$ as the probability distribution.

Now, multiplying by arbitrary function f and integrating, we see

$$\int_0^L (\sigma - \mathcal{A})[\mathcal{K}(x,y)]f(y)dy = \int_0^L \sigma \delta_x(y)f(y)dy.$$

Since $\mathcal{A}$ differentiates with respect to x, it can be moved outside of integration with respect to y, and by the definition of δ, we now have

$$(\sigma - \mathcal{A})\left[\int_0^L \mathcal{K}(x,y)f(y)dy\right] = \sigma f(x),$$

or, by the linearity of $\sigma - \mathcal{A}$,

$$(\sigma - \mathcal{A})\left[\frac{1}{\sigma}\int_0^L \mathcal{K}(x,y)f(y)dy\right] = f(x). \tag{21}$$

By the continuity of all of the functions involved, the fundamental theory of differential equations guarantees the uniqueness of this solution, meaning

$$(\sigma - \mathcal{A})[g](x) = f(x) \Rightarrow g(x) = \frac{1}{\sigma}\int_0^L \mathcal{K}(x,y)f(y)dy. \tag{22}$$

6.2 A Sturm-Liouville Identity

6.2.1 Lagrange's Identity and the Sturm-Liouville Operator

To find $\mathcal{K}$, we need to prove Lagrange's Identity concerning the *Sturm-Liouville operator* $\mathcal{L}$, where

$$\mathcal{L}[g](x) = (-p(x)g'(x))' + q(x)g(x) \tag{23}$$

for a twice-differentiable g in the domain of $\mathcal{L}$.

First, *Lagrange's Identity*:

$$-u\mathcal{L}[v] + v\mathcal{L}[u] = -[p(u'v - uv')]' = [pW(u,v)]' \tag{24}$$

for any twice-differentiable u, v, where W represents the *Wronskian* of u and v

$$W(u(x), v(x)) = det\begin{pmatrix} u(x) & v(x) \\ u'(x) & v'(x) \end{pmatrix} = u(x)v'(x) - u'(x)v(x).$$

Proof.

$$
\begin{aligned}
-[p(u'v - uv')]' &= -p'(u'v - uv') - p(u'v' + u''v - u'v' - uv'') \text{ by the chain rule} \\
&= p'(-u'v + uv') - p(u''v - uv'') \text{ by canceling terms} \\
&= -p'u'v + p'uv' - pu''v + puv'' \\
&= v(-p'u' - pu'') + u(p'v' + pv'') + puv - puv \\
&= v(-p'u' - pu'' + qu) + u(p'v' + pv'' - qv) \\
&= v((-pu')' + qu) - u((-pv')' + qv) \\
&= v\mathcal{L}[u] - u\mathcal{L}[v].
\end{aligned}
$$

$\square$

6.2.2 Sturm-Liouville Identity Proof

We will now prove an identity regarding the Sturm-Liouville operator on the functions of our concern; namely

$$
\mathcal{L}[g](x) = f(x) \Rightarrow g(x) = \frac{1}{C} \int_0^L G(x, y) f(y) dy \tag{25}
$$

whenever $g(0) = 0$ and $g'(L) = 0$. G and C are defined below in (32) and (34), respectively.

Proof. First, let ϕ and ψ be twice-differentiable functions in the domain of $\mathcal{L}$ such that

$$
\mathcal{L}[\phi] = \mathcal{L}[\psi] = 0, \tag{26}
$$

with the boundary conditions[2]

$$
\phi(0) = \psi'(L) = 0. \tag{27}
$$

Then

$$
\phi\mathcal{L}[g] - g\underbrace{\mathcal{L}[\phi]}_{=0} = (\phi \times f) - (g \times 0)
$$
$$
= \phi f.
$$

By Lagrange's identity from (24), we also have that

$$
\phi\mathcal{L}[g] - g\mathcal{L}[\phi] = [p(\phi'g - \phi g')]',
$$

meaning

$$
\phi f = [p(\phi'g - \phi g')]'. \tag{28}
$$

---

[2]Note that each of ϕ and ψ have just one of the two boundary conditions to which we hold g.

Also, by the same logic,
$$\psi f = [p(\psi' g - \psi g')]'. \tag{29}$$

Integrating (28), we see

$$
\begin{aligned}
\int_0^x \phi(y) f(y) dy &= \int_0^x \frac{d}{dy}[p(y)(\phi'(y)g(y) - \phi(y)g'(y))] dy \\
&= p(y)[\phi'(y)g(y) - \phi(y)g'(y)]\big|_0^x \\
&= p(x)[\phi'(x)g(x) - \phi(x)g'(x)] - p(0)[\underbrace{\phi'(0)g(0)}_{=0} - \underbrace{\phi(0)}_{=0} g'(0)] \\
&= p(x)[\phi'(x)g(x) - \phi(x)g'(x)]. \tag{30}
\end{aligned}
$$

Integrating (29) on a different interval, we see

$$
\begin{aligned}
\int_x^L \psi(y) f(y) dy &= \int_x^L \frac{d}{dy}[p(y)[\psi'(y)g(y) - \psi(y)g'(y)]] dy \\
&= p(y)[\psi'(y)g(y) - \psi(y)g'(y)]\big|_x^L \\
&= p(L)[\underbrace{\psi'(L)}_{=0} g(L) - \psi(L) \underbrace{g'(L)}_{=0}] - p(x)[\psi'(x)g(x) - \psi(x)g'(x)] \\
&= -p(x)[\psi'(x)g(x) - \psi(x)g'(x)]. \tag{31}
\end{aligned}
$$

Multiplying (30) by ψ and (31) by ϕ, then adding them, we see that

$$
\begin{aligned}
&\psi(x) \int_0^x \phi(y) f(y) dy + \phi(x) \int_x^L \psi(y) f(y) dy \\
&= p(x)[\phi'(x)g(x) - \phi(x)g'(x)]\psi(x) - p(x)[\psi'(x)g(x) - \psi(x)g'(x)]\phi(x).
\end{aligned}
$$

By defining a function G as[3]

$$G(x,y) = \begin{cases} \psi(x)\phi(y), & y \in [0, x) \\ \psi(y)\phi(x), & y \in [x, L], \end{cases} \tag{32}$$

we can now our previous statement to

$$\int_0^L G(x,y) f(y) dy = \underbrace{p(x)[\phi'(x)g(x) - \phi(x)g'(x)]\psi(x) - p(x)[\psi'(x)g(x) - \psi(x)g'(x)]\phi(x)}_{=Cg(x)}.$$
$$\tag{33}$$

We will now show that the term on the right side of (33) is a scalar multiple of g.

---

[3]Note that G is continuous, because $\lim\limits_{y \to x^-} G(x,y) = \lim\limits_{y \to x^+} G = G(x,x)$.

19

$$p[\phi'g - \phi g']\psi - p[\psi'g - \psi g']\phi = pg(\phi'\psi - \phi\psi') + pg'(\underbrace{-\phi\psi + \phi\psi}_{=0})$$
$$= -pg(\phi\psi' - \psi\phi')$$
$$= g \times \underbrace{(-pW(\phi,\psi))}_{=C(x)}.$$

To show that $C(x)$ is indeed a constant, we take its derivative:

$$-C' = (pW(\phi,\psi))' = p'(\phi\psi' - \phi'\psi) + p(\phi'\psi' + \phi\psi'' - \phi''\psi - \phi'\psi')$$
$$= p'(\phi\psi' - \phi'\psi) + p(\phi\psi'' - \phi''\psi)$$
$$= \phi(p'\psi' + p\psi'') - \psi(p'\phi' - p\phi'') \underbrace{+q\phi\psi - q\phi\psi}_{+0}$$
$$= \phi[(p\psi')' + q\psi] - \psi[(p\phi') + q\phi]$$
$$= \phi \underbrace{\mathcal{L}[\psi]}_{= \text{ 0 by (26)}} -\psi \underbrace{\mathcal{L}[\phi]}_{= \text{ 0 by (26)}}$$
$$= 0.$$

By (26), terms cancel, and we see that $C'(x) = 0$, and thus C is indeed a constant, written

$$C = -pW(\phi,\psi) \tag{34}$$

Now, (33) becomes

$$\int_0^L G(x,y)f(y)dy = Cg(x),$$

and we conclude

$$\mathcal{L}[g](x) = f(x) \Rightarrow g(x) = \frac{1}{C}\int_0^L G(x,y)f(y)dy, \tag{35}$$

which is (25), and we are done. $\qquad\square$

6.3   Defining ϕ and ψ explicitly

For completeness, solving for ϕ and ψ will be outlined.

The general solution to the differential equation

$$\mathcal{L}[f] = (-pf')' + qf = 0$$

with p and q defined in (41) and (42), yields the solution

$$f(x) = e^{\frac{v}{2D}x}(c_1 e^{irx} + c_2 e^{-irx}),$$

where
$$r = \frac{\sqrt{-(\frac{v}{D})^2 - 4\sigma D}}{2}.$$ (36)

In the case of ϕ, a solution to $\mathcal{L}[\phi] = 0$, the boundary condition $\phi(0) = 0$ implies that $c_2 = -c_1$, leaving us with

$$\phi(x) = ce^{\frac{v}{2D}x}(e^{irx} - e^{-irx}) = ce^{\frac{v}{2D}x}sin(rx),$$ (37)

with r defined in (36).

In the case of ψ, another solution to $\mathcal{L}[\psi] = 0$, the boundary condition that $\psi'(L) = 0$ implies, with a bit of algebra, that CHECK THIS CHECK THIS CHECK THIS!

$$c_2 = -c_1 e^{2irL}\left(\frac{v + 2Dir}{v - 2Dir}\right),$$

leaving us with

$$\psi(x) = ce^{\frac{v}{2D}x}(e^{irx} - e^{2irL}\left(\frac{v + 2Dir}{v - 2Dir}\right)e^{-irx}),$$ (38)

with r defined in (36).

It is worth noting that in the final solution of $\mathcal{K}$, there are terms C and G, which are left in terms of particular solutions to to differential equations ϕ and ψ. However, in the final formulation of the kernel, we have $\mathcal{K} \propto \frac{G}{C}$, and both G and C are proportional to $(c_\phi \times c_\psi)$, those being the coefficients of whatever specific solutions are chosen. Thus, $\mathcal{K}$ can be given in terms of arbitrary specific solutions or general solutions without affecting the values (that is, any chosen values of c_ϕ and c_ψ on ϕ and ψ are irrelevant).

6.4   Direct Definition of $\mathcal{K}$

We have shown in (6.1) and (6.2) that for any twice-differentiable g in the domain of $(\sigma - \mathcal{A})$ and $\mathcal{L}$, which are the operators defined by

$$(\sigma - \mathcal{A})[g] = \sigma g - Dg'' + vg',$$
$$\mathcal{L}[g] = (-pg')' + qg$$

we have

$$(\sigma - \mathcal{A})[g](x) = f(x) \Rightarrow g(x) = \frac{1}{\sigma}\int_0^L \mathcal{K}(x, y)f(y)dy$$ (39)

$$\mathcal{L}[g](x) = f(x) \Rightarrow g(x) = \frac{1}{C}\int_0^L G(x, y)f(y)dy.$$ (40)

To start we explicitly define

$$p(x) = e^{\frac{-v}{d}x}$$ (41)

$$q(x) = \frac{\sigma}{D}e^{\frac{-v}{d}x} = \frac{\sigma}{D}p(x).$$ (42)

21

Now let g be a function in the proper domain such that $\mathcal{L}[g](x) = f(x)$. That means

$$
\begin{aligned}
f = \mathcal{L}[g] &= (-pg')' + qg \\
&= qg - p'g' - pg'' \\
&= \frac{\sigma}{D}e^{\frac{-v}{D}x} - e^{\frac{-v}{D}x}g'' + \frac{v}{D}e^{\frac{-v}{D}x}g' \\
&= \frac{1}{D}e^{\frac{-v}{D}x}(\sigma g - Dg'' + vg') \\
&= \frac{1}{D}p \times (\sigma - \mathcal{A})[g].
\end{aligned}
$$

Putting this all together,

$$(\sigma - \mathcal{A})[g](x) = \frac{Df(x)}{p(x)}. \tag{43}$$

Now, by (39), we see that (43) tells us that

$$g(x) = \frac{1}{\sigma}\int_0^L \mathcal{K}(x, y)\frac{Df(y)}{p(y)}dy.$$

On the other hand, since $\mathcal{L}[g](x) = f(x)$, (40) tells us that

$$g(x) = \frac{1}{C}\int_0^L G(x, y)f(y)dy.$$

Putting this all together, we have

$$\frac{1}{\sigma}\int_0^L \mathcal{K}(x, y)\frac{Df(y)}{p(y)}dy = \frac{1}{C}\int_0^L G(x, y)f(y)dy.$$

Since this is true for all f such that $\mathcal{L}[g] = f$ for some g, which can basically be any function, the integral and the arbitrary function can be omitted[4] to conclude

$$\mathcal{K}(x, y)\frac{D}{\sigma p(y)} = \frac{1}{C}G(x, y).$$

or simply

$$\mathcal{K}(x, y) = \frac{\sigma p(y)}{CD}G(x, y) \tag{44}$$

with p, C, and G defined in (41), (34), and (32), respectively.

---

[4]Leaving aside the issue as to whether or not $\mathcal{L}[g]$ can equal such functions, suppose $\mathcal{L}[g] = \delta_\xi, \xi \in [0, L]$ (Delta function). Then the integral with $f(y) = \delta_\xi(y)$ results in the desired equality (the equality without f and without the integral: equation (44)). Furthermore, assuming a reasonably broad algebra of functions (see Stone-Weierstrass Thm. conditions) are solutions to $\mathcal{L}[g] = f$, and that sufficient linear combinations and products of them are also solutions, then there exists a solution f that arbitrarily approximates δ_ξ for any ξ and thus δ_ξ can be said to be a value of $\mathcal{L}[g]$ for some g.

7 Appendix C

7.1 Stopping-Time Probability Derivation

The following outlines the method by which our model to predict the likelihood of an individual having transitioned from a point x on a river stretch to point 0 after time t. As will be shown, the interest is in the 'stopping time' H_0, a random variable denoting the length of time until another random variable completes a stochastic trajectory.

We examine a changing probability distribution $u(y,t)$ denoting the probability of a particle existing at location $y < L$ at time t subject to the following condition:

$$\frac{\partial u}{\partial t}(y,t) = \mathcal{A}_y[u](y,t) = D\frac{\partial^2 u}{\partial y^2}(y,t) - v\frac{\partial u}{\partial y}(y,t) \tag{45}$$

$$u(y,0) = u_0(y)$$

$$u(0,t) = f(t)$$

We use Dynkin's formula, which states the equivalence of the probability of existingg at y after time t, denoted $u(y,t)$, with that of *arriving at an initial position through the equivalent backwards process (arriving at a given location at $t = 0$)*[5]:

$$u(y,t) = \mathbb{E}_{X(0)=y}[u_0(X_t) \times \mathbb{1}(t < H_0) + f(t - H_0) \times \mathbb{1}(t > H_0)] \tag{46}$$

where

- $u_0(x) = u(x,0)$, the given distribution of probability of location of an individual at time $t = 0$;

- $\mathbb{1}(b) = \begin{cases} 1, & b \text{ is true} \\ 0, & b \text{ is false} \end{cases}$, an indicator function;

- $X(t)$ is a random variable denoting a location at time t, meaning $\mathbb{P}(X(t) = y) = u(y,t)$;

- H_0 denotes the *stopping time* of the random variable $X(t)$; that is, H_0 is a random variable denoting the length of time until $X(t) = 0$ to end its 'random walk'. As we will see, we are interested in $\mathbb{P}(H_0 \in dt)$.

A probabilistic analysis of (45) and (46) under these conditions yields that[6]

---

[5]The 'backwards process' is a stochastic trajectory between two spatio-temporal points in the backwards time direction such that the probability of traveling along a given path is equal to the likelihood of traveling along that same path in the forwards process being modeled.

[6]The complexity of this derivation is beyond the scope of this paper, but it follows from the definition of expected value.

$$u(y,t) = \int_0^L u_0(x)P(y,x,t)dx + \int_0^t f(t-s)\mathbb{P}(H_0 \in ds)ds \qquad (47)$$

where $P(y,x,t)$ denotes the probability density of completing a transition from x to y at time t and is the solution to the backwards advection-diffusion equation with absorbing boundary condition $P(0,x,t) = P(y,0,t) = 0$; a direct expression for P is omitted but can be found in Borodin and Paavo's *Handbook of Brownian Motion*.

Next, we analyze another quantity in two ways to obtain another expression for $u(y,t)$:

$$I = \int_0^t \int_0^\infty \frac{\partial}{\partial t}[P(y,x,t-s)u(x,s)]dxds$$

$$= \int_0^\infty \int_0^t \frac{\partial}{\partial t}[P(y,x,t-s)u(x,s)]dsdx$$

$$= \int_0^\infty P(y,x,0)u(x,t) - P(y,x,t)u(x,0)dx$$

Noting the P(y,x,0) is equal to the delta function allows us to rewrite the above expression

$$I = u(y,t) - \int_0^L P(y,x,t)u_0(x)dx. \qquad (48)$$

On the other hand, by the product rule we may also write[7]

$$I = \int_0^t \int_0^\infty \frac{\partial}{\partial t}P(y,x,t-s)u(x,s) + P(y,x,t-s)\frac{\partial}{\partial t}u(x,t)dxds$$

$$= \int_0^t \int_0^\infty -\left(D\frac{\partial^2 P}{\partial x^2} + v\frac{\partial P}{\partial x}\right)u(x,s) + P(y,x,t-s)\left(\frac{\partial^2 u}{\partial x^2} - v\frac{\partial u}{\partial x}\right)dxds$$

$$= \int_0^t \frac{\partial P}{\partial x}(y,0,t-s)u(x,s) - D\frac{\partial}{\partial x}u(0,s)P(y,0,t-s) + vP(y,0,t-s)u(0,s)ds$$

$$= \int_0^t D\frac{\partial P}{\partial x}(y,0,t-s)f(s)ds$$

$$= \int_0^t D\frac{\partial P}{\partial x}(y,0,s)f(t-s)ds. \qquad (49)$$

Putting (48) and (49) together, we see that

$$\int_0^t D\frac{\partial}{\partial x}P(y,0,s)f(t-s)ds = u(y,t) - \int_0^L P(y,x,t)u_0(x)dx$$

$$\Rightarrow u(y,t) = \int_0^t D\frac{\partial P}{\partial x}(y,0,s)f(t-s)ds + \int_0^L P(y,x,t)u_0(x)dx. \qquad (50)$$

---

[7]Here we change variables from s to $t-s$ which, after changing the differential and limits of integration, amounts to this equation's final form.

Now, putting (47) and (50) together, we see that

$$\int_0^t Df(t-s)\frac{\partial P}{\partial x}(y,0,s)ds + \int_0^L u_0(x)P(y,x,t)dx = \int_0^t f(t-s)\mathbb{P}(H_0 \in ds)ds + \int_0^L u_0(x)P(y,x,t)dx$$

$$\Rightarrow \mathbb{P}(H_0 \in ds) = D\frac{\partial P}{\partial x}(y,0,s), \tag{51}$$

giving a direct expression for $\mathbb{P}(H_0 \in ds)$.

7.2 Determination of Parameters Using Stopping-Time

The percentage of tracers collected in the stream experiment in section (2.3) corresponds to the likelihood of a tracer having transitioned a given distance after a given time. Specifically, letting $N(x,t)$ denote the percentage of tracers collected at distance 0 after being released from distance x and after an elapsed time t, we can state that

$$N(x,t) = \left(\int_0^t \mathbb{P}(H_0 \in ds)ds\right)[x], \tag{52}$$

which can be intuitively understood to mean that the likelihood of having from x to 0 by time t is equal to the integral of the probability of that transition happening at a given unit time over all possible units of time between 0 and t.

As the direct formula for $\mathbb{P}(H_0 \in ds)$ is in terms of parameters v and D representing advection velocity and diffusion, respectively, measured values of $N(x_i, t_j)$ can be used to determine the real values of those parameters within the model. Specifically, the values of D and v such that

$$\sum_i \sum_j \left((N(x_i, t_j) - \left(\int_0^{t_j} \mathbb{P}(H_0 \in ds)ds\right)[x_i]\right)^2$$

is minimized are presumed to be the 'real' values of v and D.

While this is the only way to determine D, a descriptive parameter, v, the advection velocity, can be assumed to be roughly equal to the velocity of the current in which the experiment took place. Thus, the validity of the claim on the 'real' values of D and v can be cross-checked against reality.

References

[1] Allan JD, Feifarek BP. 1989. Distances traveled by drifting mayfly nymphs: factors influencing return to the substrate. *Jour. of the N. Amer. Benth. Soc.* 8(4):322-330.

[2] "Andrews Experimental Forest LTER: Watershed 3 - WS03". *Andrews Experimental Forest LTER.* 2011. Web. 6 Aug. 2012. >

[3] Breitenmoser-Wursten C, Sartori M. 1994. Distribution, diversity, life cycle and growth of a mayfly community in a prealpine stream system (Insect, Ephemeroptera). *Hydrobiologia.* 308:85-101.

[4] Encalada AC, Peckarsky BL. 2005. Selective oviposition of the mayfly Baetis bicaudatus. *Oecologia.* 148: 526-537.

[5] Gibbons CN, Batalla RJ, Vericat D. 2010. Relations between invertebrate drift and flow velocity in sand-bed and riffle habitats and the limits imposed by substrate stability and benthic density. *Jour. of the N. Amer. Benth. Soc.* 29(3):945-958.

[6] Huryn AD, Wallace JB. 2000. Life history and production of stream insects. *Annu. Rev. Entomol.* 45:83-110.

[7] Lutscher F, Pachepsky E, Lewis MA. 2005. The effect of dispersal patterns on stream populations. *SIAM J. Appl. Math.* 65(4):1305-1327.

[8] Ramirez JM. 2011. Population persistence under advection-diffusion in river networks. *J. Math. Biol.* Online.

[9] Waters TF. 1972. The drift of stream insects. *Annu. Rev. Entomol.* 17:253-272.

[10] Borodin, A. N., and Paavo Salminen. Handbook of Brownian Motion: Facts and Formulae. Basel: Birkhuser Verlag, 1996. Print.